A GLOBAL MODELING PROGRAM FOR CO-ROTATING TWIN-SCREW EXTRUDERS

C. Teixeira, J. A. Covas and A. Gaspar-Cunha

I3N / IPC – Institute for Polymers and Composites, Department of Polymer Engineering, University of Minho, Guimarães, Portugal - denebe@dep.uminho.pt, agc@dep.uminho.pt, jcovas@dep.uminho.pt

Abstract - A global plasticating modeling software for twin screw extruders is presented. The program computes the evolution of pressure, average and maximum temperature, shear rate, viscosity, mechanical power consumption, degree of fill, residence time and mixing along a sequence of the various elements (conveying, left handed and kneading blocks) that are used to assemble a typical screw. Modeling is performed from hopper to die, considering solids conveying, melting and melt flow and takes into account the geometrical characteristics of each screw element. The effect of the operating conditions and screw geometry on the flow were compared with experimental data.

Introduction

Intermeshing co-rotating twin-screw extruders are commonly used by the polymer, pharmaceutics and food industries for processing, compounding and reactive extrusion operations, due to their construction flexibility, mixing capabilities, and output and residence time control.

However, flow and heat transfer inside these machines is quite complex, and is significantly affected when the screw profile is modified (e.g. by varying the number and/or the geometry of kneading blocks), or the operating conditions are changed (barrel temperatures, output, screw speed). Not surprisingly, modelling the flow in these machines has been attempted, either describing the overall process based on simplified flow assumptions, or describing in detail the complex 3D flow in specific mixing sections (Potente and Melish, 1996; Vergnes *et al.*, 1998; White *et al.*, 2001).

This work presents a modelling routine that takes into consideration the main process steps from hopper to die, by adopting individual models available in the literature and coupling them in a coherent way. The steps include: i) starve fed solids conveying, ii) non-isothermal solids conveying under pressure, iii) flow of a solid plug separated from the barrel by a melt film, iv) melting of a solid bed surrounded by melt films, v) melting of particles suspended in a melt, vi) non-isothermal melt conveying under pressure, and vi) melt conveying without pressure. The program computes the evolution along the screws of pressure, temperature, mechanical power consumption, shear rate, viscosity, residence time and filling ratio. The predictions are compared with experimental measurements. The response of the system to changes in the main process variables is investigated.

Process Modeling

Geometry

Given the geometrical complexity of the screws used in co-rotating twin-screw extruders, it is important to introduce simplifications than can avoid the need to perform expensive 3D computations. The following types of screw elements are considered:

i) Conveying, or right handed elements, having a positive helix angle and, consequently, high conveying capacity;
ii) Left handed elements, having a negative helix angle and, thus, restricting the flow;
iii) Kneading blocks, combining various kneading discs, with the possibility of creating different staggering angles. Blocks with positive staggering have good conveying capacity. Neutral or orthogonal blocks have no axial drag. Negative staggering angles can be highly restrictive, but they generate intensive mixing, and promote efficient heat.

Figure 1 shows a right handed screw section, using double flighted screw elements. The cross-section is converted into an equivalent rectangular channel with the same cross-sectional area (Booy, 1978; Rauwendal, 1986; White, 1990), fixing the height as $H_{max}/2$. Figure 2 depicts a kneading block and shows that the staggering angle forms two major flow channels, Q_C and Q_L, with positive and negative drag, respectively, both approximately rectangular but with different widths. In each channel, the flow is similar to that developing in right or left handed elements, (Booy, 1978; Vergnes *et al.,* 1998).

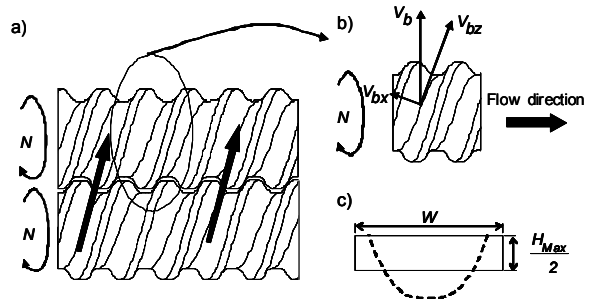

Figure 1- Geometry and flow in right-handed screw elements.

Individual Modeling Steps

The sequence and extension of each process step depends on the screw configuration and operating conditions. Even so, Figure 3 illustrates a typical series: 1) solids conveying without pressure, 2) solids conveying under pressure, 3) melting; 4) melt conveying under pressure and 5) melt conveying without pressure.
As soon as the material reaches the first restrictive element, pressure builds up and melting develops very quickly (White, 1990).
The corresponding individual models were linked together in a global model using coherent boundary conditions.

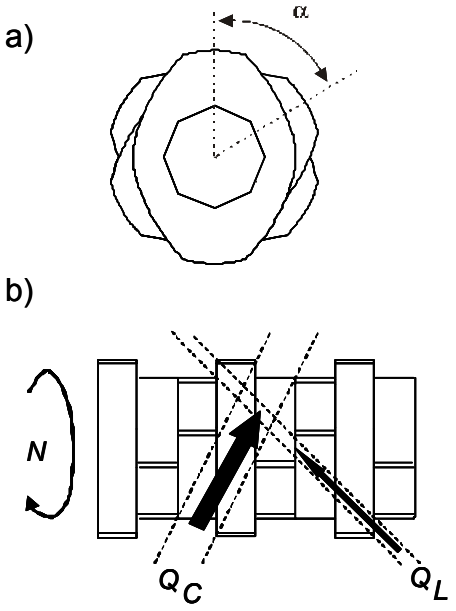

Figure 2- Geometry and flow in a kneading block.

Computer modeling

The global algorithm flowchart is presented in Fig. 4. The operating conditions (screw speed, output, barrel temperature profile), material properties and screw and die geometries are defined. Calculations progress from the screw entrance to the die exit.

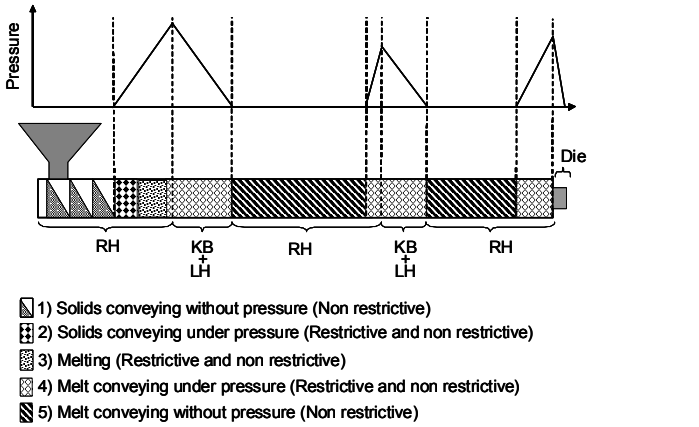

Figure 3- Process steps in a co-rotating twin-screw extruder (RH – Rigth handed elements; LH- Left

The program starts by assessing the restrictive character of all screw elements. Then, flow calculations begin at the first restrictive element, an iterative procedure being used to identify the location upstream, L_0, where the channel becomes fully filled. Calculations can now be performed along small Δz channel increments. During flow along the first restrictive element solids conveying, delay, melting and melt conveying are included, while later only melt conveying becomes relevant.
This iterative process is repeated for every restrictive element. In the case of partially filled sections, only the temperature evolution is computed.

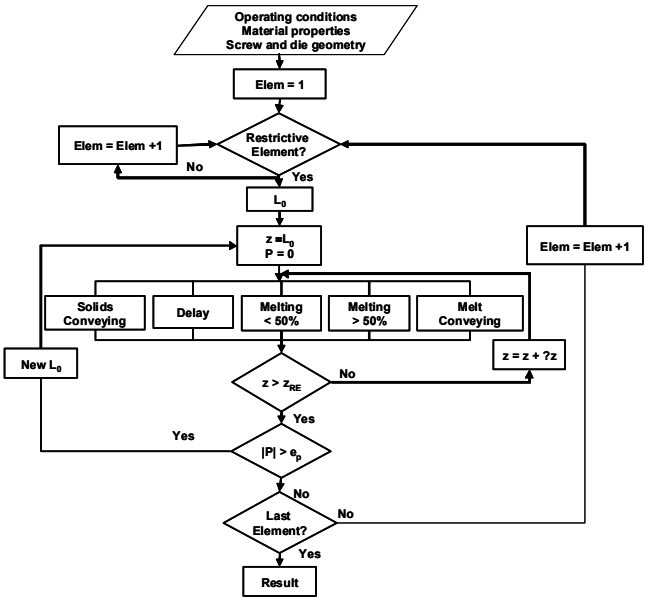

Figure 4- Modeling flowchart.

Case Study

In order to compare model predictions with experimental results, a laboratorial Leistritz LSM 30.34 co-rotating twin screw extruder was used. Figure 5 and Table 1 show the layout, screw configuration, and the location of sampling devices that were used to measure

real melt temperatures (Carneiro *et al*, 2000). ISPLEN PP030 G1E, a polypropylene manufactured by Repsol, has the properties summarized in Table 2.

Table 1- Screw profile (a negative pitch indicates a left handed element and a KD-30º denotes a block of left handed kneading discs with a staggering angle of -30º).

Screw Element	**1**	**2**	**3**	**4**	**5**	**6**	**7**	**8**
Length (mm)	97.5	120	60	30	60	30	120	60
Pitch (mm)	45	30	30	30	KD -30º	60	30	20
Screw Element	**9**	**10**	**11**	**12**	**13**	**14**	**15**	**16**
Length (mm)	30	120	60	60	22.5	30	30	30
Pitch (mm)	KD -60º	60	45	30	KD 30º	-20	30	20

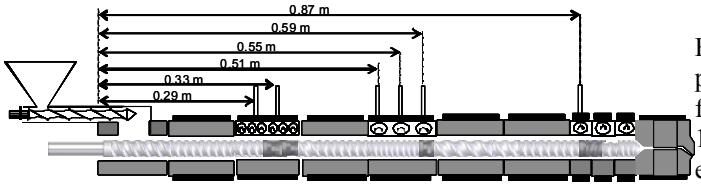

Figure 5- Geometrical description of twin-screw extruder and location of the pressure transducers.

Table 2- Polymer properties.

			PP (ISPLEN PP 030 G1E)	
Density	Solids	ρ_s	690.90	$kg.m^{-3}$
	Melt	ρ	902.00	
Thermal Conductivity	Solids	k_s	0.21	$W.m^{-1.o}C^{-1}$
	Melt	k_m	0.18	
Specific Heat	Solids	C_s	1881.92	$J.kg^{-1}$
	Melt	C_m	1974.55	
Melting	Heat	H	$89.49x10^3$	$J.kg^{-1}$
	Temp.	T_m	170	^oC
Viscosity Carreau-Yasuda law		η_0	3041.48	$Pa.s$
		E/R	4023.29	K
		$\hat{\lambda}$	0.17	s
		a	1.82	
		n	0.35	
		T_0	493.15	K

The following parameters were measured experimentally: output, melt temperature (directly on the melt), pressure, fill ratio, mechanical power consumption and residence time distribution. The mechanical power consumption was estimated from the value of the current intensity measured (Rauwendall, 1986). The residence time was estimated trough the use of pigment as a tracer. For that, various samples were collected at the die for time intervals (Δt) of 10 s. Then each sample was classified accordingly with the pigment concentration and the average residence time was calculated.

Concerning computer calculations, different runs were performed in order to study the sensibility of the software to changes in the operating conditions (e.g., screw speed, output and barrel temperature profile). The output ranges between 4 and 12 kg/h, the screw speed ranges between 100 and 200 rpm and the barrel temperature profile ranges between 205 and 235 ºC.

Results

General results

Figure 6 shows the computational and experimental pressure and temperature profiles along the extruder for a run with an output of 8kg/hr, a screw speed of 150rpm and a barrel temperature of 220ºC. As expected, the pressure starts to develop in the screw element before the location of the different restrictive elements (5, 9 and 13/14, see Table 1) and before the die. This is due to the flow constraint imposed by the presence of these types of elements. The maximum pressure is obtained at the beginning of the restrictive elements and at the beginning of the die. As can be seen, the temperature increases under pressure conditions mainly due to viscosity dissipation and due to the efficiency of heat conduction from the barrel, since the contact between the polymer and the barrel is higher. In partially filled channels the temperature decreases since the barrel is at lower temperature. The computed results have an identical behavior than those of the experimental ones. The first three values of temperature are an exception, since they are over estimated, probably due to the presence of solid material in these locations were the temperature was measured.

Figure 7 presents the local and cumulative residence time computed along the screw for the same run. The cumulative residence time calculated was compared with the average residence time obtained experimentally (single dot on the figure). The differences are not important. As expected, the local residence time is higher in the restrictive elements, i.e., in the presence of kneading blocks and left handed elements. An important observation is that the local residence time is very sensitive to the geometry of each screw element. As expected, lower values for local residence time in right handed elements with higher

pitch and higher values for restrictive elements have been obtained.

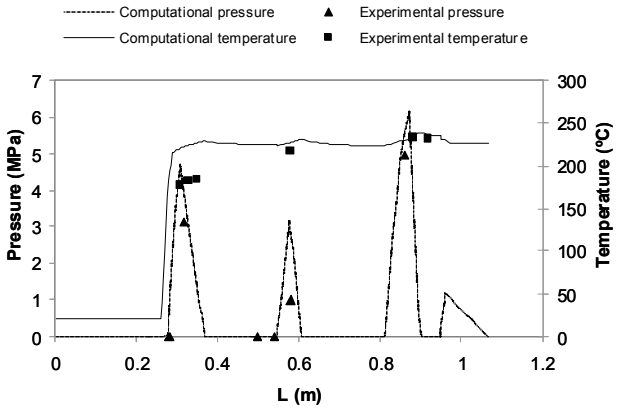

Figure 6- Comparison between computational and experimental temperature and pressure profiles for run1.

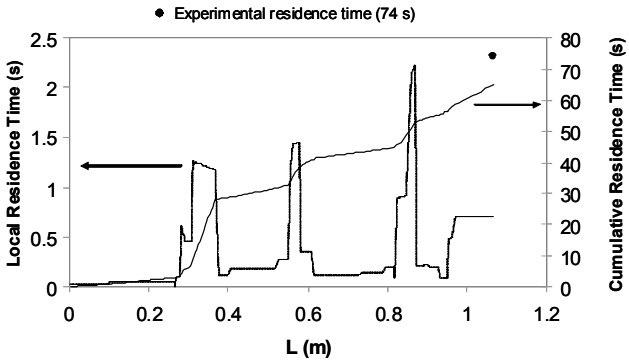

Figure 7- Local and cumulative residence time predicted along screws and die and residence time measured.

Influence of screw speed

Figures 8 to 11 and Table 3 presents the results obtained (computational and experimentally) for changes on screw speed (100, 150 and 200 rpm). The polymer temperature (Figure 8) is higher for higher screw speeds due to higher viscosity dissipation induced. However, at the beginning, the temperature computed is higher for low screw speed, since in this case the melting starts first, and only when melting starts the temperature is computed. The higher differences between the experimental and computational results obtained at the first three measure locations are due to the presence of solid material that difficult the measurements.

Table 3 shows the values calculated for different parameters: i) length needed for melting, form the beginning of the melting phase; ii) location for total melting, representing the total length from the bottom of the hopper and iii) length of channel totally filled before the first restrictive element where melting takes place. Increasing screw speed implies that the totally filled channel length before the restrictive element decreases (Table 3). Thus melting is delayed, since heat conduction is less efficient due to the lower residence time (Figure 9), as a consequence, the melting process finishes later but is faster (Table 3). The average of the shear rate along the screw axis for different values of screw speed is represented in Figure 10. As expected, higher value of shear rate is obtained for higher values of screw speed.

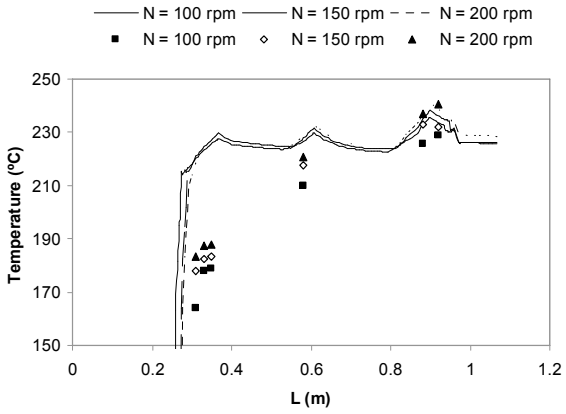

Figure 8- Comparison between computed and measured temperature different values of screw speed.

Table 3– Influence of screw speed on melting process and fill ratio (* before restrictive element).

Screw speed (rpm)	**100**	**150**	**200**
Length needed for melting (mm)	27.8	26.5	26.3
Location of total melting (mm)	277.5	288.7	292.5
Length for channel totally filled (mm)*	57	45.3	42.2

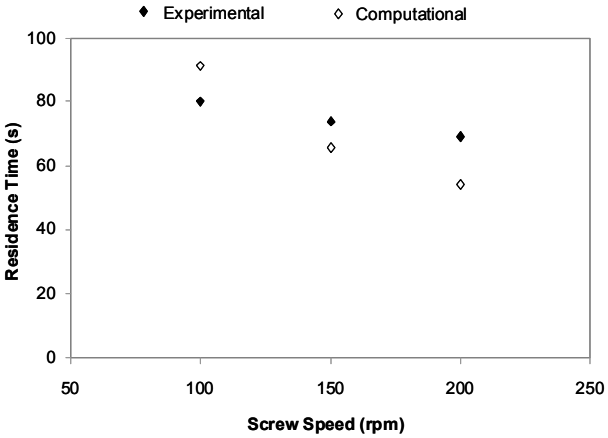

Figure 9- Comparison between measured and computed residence time for different values of screw speed.

Finally, the comparison between the computational and the experimental pressure results (Figure 11) allows one to conclude that the influence of screw speed is very identical in both cases. For the different screw speeds only some differences exist at maximum pressure location.

Identical runs were made for studying the influence of output, barrel temperature and screw configuration.

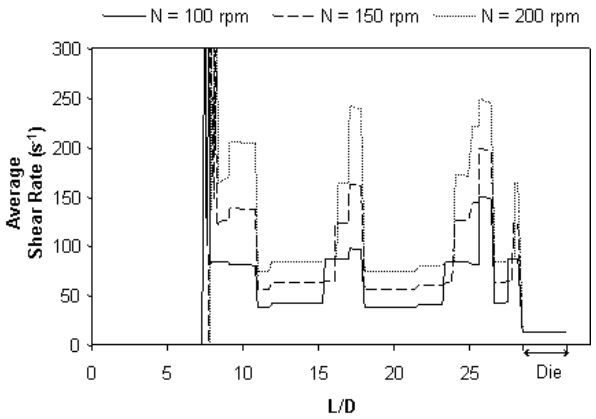

Figure 10- Evolution of average shear rate along the screw for different values of screw speed.

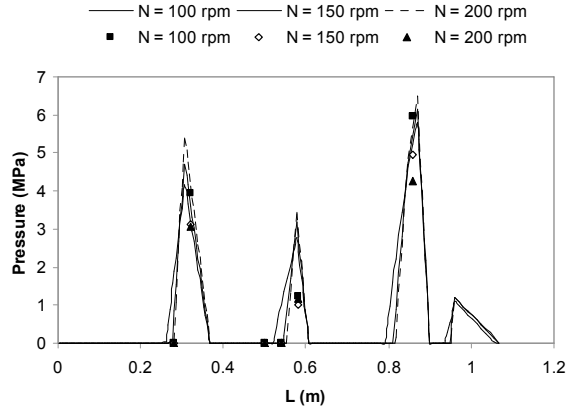

Figure 11- Comparison between computed and measured pressure for different values of screw speed.

Conclusions

A global plasticating modeling software for twin screw extruders has been presented. The computed results were directly compared with experimental data and the influence of operating conditions and screw geometry in different parameters were studied.

The global modeling program presented is able to model the extrusion process from the hopper until the end of die in a reasonable computational time (1 to 2 minutes in a personable computer – Pentium M 1.75 GHz).

The software is able to predict the evolution of pressure, temperature, residence time, fill ratio and mechanical power consumption along a sequence of different screw elements. It is sensitive to variations of operating conditions: screw speed, output and barrel temperature; and it takes into account the geometrical particularities of different screw elements.

The results are in agreement with theoretical and experimental knowledge.

Acknowledgements

The authors are grateful to Portuguese Fundação para a Ciência e Tecnologia for supporting this work under grant SFRH/BD//21921/2005.

References

H. Potente, U. Melisch, “Theoretical and Experimental Investigations of the Melting of Pellets in Co-Rotating Twin Screw Extruders”, International Polymer Processing, XI, p. 101-108, 1996.

B. Vergnes, G. Della Valle, L. Delamare, “A Global Computer Software for Polymer Flows in Corotating Twin Screw Extruders”, Polymer Engineering and Science, 38, p. 1781-1792, 1998.

J. L. White, B. Kim, S. Bawiskar, J. M. Keum, “Development of a Global Computer Software for Modular Self-Wiping Corotating Twin Screw Extruders”, Polymer-Plastics Technology and Engineering, 40, p. 385-405, 2001.

M. L. Booy, “Geometry of Fully Wiped Twin-Screw Equipment”, Polymer Engineering and Science, 18, p. 973-984, 1978.

C. Rauwendaal, Polymer Extrusion, Hanser Publishers, Munich ,1986.

J.L. White, “Twin Screw Extrusion; Technology and Principles”, Hanser, Munich, 1990.

O. S. Carneiro, J. A. Covas, B. Vergnes, Experimental and Theoretical Study of Twin Screw Extrusion of Polypropylene. J. Appl. Polym. Sci., **78**, 1419-1430, 2000.